Large mode area silicon microstructured fiber with robust dual mode guidance

N. Healy[1], J. R. Sparks[2], M. N. Petrovich[1], P. J. A. Sazio[1], J. V. Badding[2], and A. C. Peacock[1]

[1] *Optoelectronics Research Centre, University of Southampton, Southampton SO17 1BJ, UK*
[2] *Department of Chemistry and Materials Research Institute, Pennsylvania State University, 16802 PA, USA*

acp@orc.soton.ac.uk

Abstract: A silicon microstructured fiber has been designed and fabricated using a pure silica photonic bandgap guiding fiber as a 3D template for materials deposition. The resulting silicon fiber has a micron sized core but with a small core-cladding index contrast so that it only supports two guided modes. It will be shown that by using the microstructured template this fiber exhibits a number of similar guiding properties to the more traditional index guiding air-silica structures. The large mode areas and low optical losses measured for the silicon microstructured fiber demonstrate its potential to be integrated with existing fiber infrastructures.

OCIS codes: (060.2280) Fiber design and fabrication; (060.2290) Fiber materials; (160.6000) Semiconductor materials; (190.4370) Nonlinear optics, fibers

References and links

1. B. Jalali and S. Fathpour, "Silicon Photonics," J. Lightwave Technol. **24**, 4600–4615 (2006).
2. M. A. Foster, K. D. Moll, and A. L. Gaeta, "Optical waveguide dimensions for nonlinear interactions," Opt. Express **12**, 2880–2887 (2004).
3. M. Lipson, "Overcoming the limitations of microelectronics using Si nanophotonics: solving the coupling, modulation and switching challenges," Nanotechnology **15**, S622–S627 (2004).
4. P. J. A. Sazio, A. Amezcua-Correa, C. E. Finlayson, J. R. Hayes, T. J. Scheidemantel, N. F. Baril, B. R. Jackson, D.-J. Won, F. Zhang, E. R. Margine, V. Gopalan, V. H. Crespi, and J. V. Badding, "Microstructured Optical Fibers as High-Pressure Microfluidic Reactors," Science **311**, 1583–1586 (2006).
5. J. C. Knight, "Photonic crystal fibres," Nature **424**, 847–851 (2003).
6. V. Raghunathan, D. Borlaug, R. R. Rice, and B. Jalali, "Demonstration of a Mid-infrared silicon Raman amplifier," Opt. Express **15**, 14355–14362 (2007).
7. V. Raghunathan, H. Renner, R. R. Rice, and B. Jalali, "Self-imaging silicon Raman amplifier," Opt. Express **15**, 3396–3408 (2007).
8. L. Yin, Q. Lin, and G. P. Agrawal, "Soliton fission and supercontinuum generation in silicon waveguides," Opt. Lett. **32**, 391–393 (2007).
9. T. M. Monro and D. J. Richardson, "Holey optical fibres: Fundamental properties and device applications," Comptes Rendus Physique **4**, 175–186 (2003).
10. M. N. Petrovich, F. Poletti, A. van Brakel, and D. J. Richardson, "Robustly single mode hollow core photonic bandgap fiber," Opt. Express **16**, 4337–4346 (2008).
11. C. R. Kurkjian, J. T. Krause, and M. J. Matthewson, "Strength and Fatigue of Silica Optical Fibers," J. Ligthwave Technol. **7**, 1360–1370 (1989).
12. L. Lagonigro, N. V. Healy, J. R. Sparks, N. F. Baril, P. J. A. Sazio, J. V. Badding, and A. C. Peacock, "Wavelength-dependent loss measurements in polysilicon modified optical fibres," CLEO/Europe-EQEC **CE3** (2009).
13. T. A. Birks, J. C. Knight, and P. St. J. Russell, "Endlessly single-mode photonic crystal fiber," Opt. Lett. **22**, 961–963 (1997).
14. L. Liao, D. R. Lim, A. M. Agarwal, X. Duan, K. K. Lee, and L. C. Kimerling, "Optical Transmission Losses in Polycrystalline Silicon Strip Waveguides: Effects of Waveguide Dimensions, Thermal Treatment, Hydrogen Passivation, and Wavelength," J. Electron. Mater. **29**, 1380–1386 (2000).

#114924 - $15.00 USD Received 28 Jul 2009; revised 28 Aug 2009; accepted 15 Sep 2009; published 23 Sep 2009

15. C. E. Finlayson, A. Amezcua-Correa, P. J. A. Sazio, N. F. Baril, and J. V. Badding, "Electrical and Raman characterization of silicon and germanium-filled microstructured optical fibers," Appl. Phys. Lett. **90**, 132110 (2007).
16. G. Cocorullo, F. G. Della Corte, R. De Rosa, I. Rendina, A. Rubino, and E. Terzini, "Amorphous Silicon-Based Guided-Wave Passive and Active Devices for Silicon Integrated Optoelectronics," IEEE J. Sel. Top Quant. **4** 997–1002 (1998).

1. Introduction

The burgeoning field of silicon photonics owes much of its success from the ability to leverage a vast, highly developed and capitalized microelectronics industry that allows for deep sub-micron lithographic processes at a wafer scale [1]. Typical on-chip silicon photonic devices are constructed by defining waveguiding structures on silicon-on-insulator (SOI) wafers that were originally developed to minimize the parasitic capacitance of high speed electronic devices such as heterojunction bipolar transistors. Recently, there has been increased interest in tailoring the waveguide design to optimize these devices for photonics applications [2]. As the high core-cladding index contrast results in strong optical confinement, so that waveguides of micron-scale dimensions are highly multimoded, attentions have primarily focused on scaling down the core to nanometer dimensions [3]. Such scaling not only reduces the number of guided modes supported by the core, thus reducing mode competition, but also increases the field intensities. Unfortunately, however, this approach limits the optical power that can be launched into these structures before damage thresholds are reached, as well as significantly reducing the coupling efficiency between devices, particularly if light is launched by an optical fiber owing to the mismatch in mode cross sections. Furthermore, small core structures force more light into the cladding, which increases losses due to surface roughness at the core-cladding interface and inhibits the use of these waveguides at wavelengths greater than $2\,\mu$m, where the optical losses in the silica cladding are large.

An alternative approach to silicon waveguide fabrication makes use of a high pressure chemical processing technique to deposit the semiconductor material into the air holes of pure silica microstructured optical fiber (MOF) templates [4]. MOFs make exceptional 3D templates for materials deposition as they are temporally and mechanically stable, and the aperiodic or periodic arrangement of air holes can be tightly controlled during the fabrication process so that by choosing an appropriate structure the spatial distribution of the optical power in the guided mode can be carefully engineered [5]. For example, by depositing silicon into a capillary with a single central air hole we can emulate the on-chip silicon-silica rib waveguides, whilst deposition in a MOF with multiple holes can offer 2D geometrical design freedom similar to that available in the pure glass MOFs themselves. In this paper we demonstrate the design, fabrication and characterization of a large core dual mode silicon microstructured fiber waveguide. This structure is realized via the complete filling of a hollow core silica photonic bandgap fiber (PBGF) with high index silicon; the central hole, now filled with silicon, still acts like the fiber's core, while the silicon rods lattice and silica webbing act as a lower effective index cladding. Thus, in doing this, we have converted the original fiber from a photonic bandgap guiding to a total internal reflection guiding waveguide.

This silicon microstuctured fiber has a comparatively large core of several microns diameter, but a very small core-cladding effective index difference so that it supports significantly fewer guided modes than an equivalently sized conventional silicon-silica structure. Thus such large mode area (LMA) silicon fibers offer improved coupling with standard micron sized single mode silica fibers compared to on-chip waveguide devices, which has previously been seen as one of the major bottlenecks to silicon device technology. Further to this, the ability to realize LMA structures that are not highly multimode has a number of additional advantages for practical device applications. For example, LMA fibers exhibit low nonlinearities, low confinement

#114924 - $15.00 USD Received 28 Jul 2009; revised 28 Aug 2009; accepted 15 Sep 2009; published 23 Sep 2009

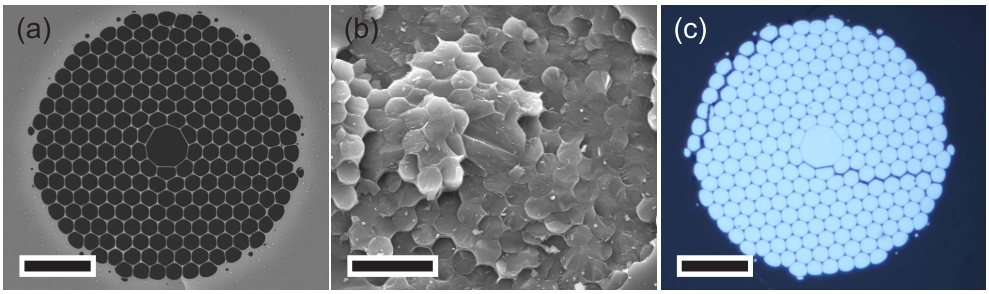

Fig. 1. (a) Silica PBGF template; scale bar 20 μm. (b) Silicon filled MOF; scale bar 10 μm. (c) Polished fiber; scale bar 20 μm.

losses, can have guidance properties that are largely wavelength independent and can tolerate very high power levels. Our investigations have shown this structure to be dual mode over a very wide wavelength range from the near to mid-infrared with losses that depend only on the material quality. The properties of this novel silicon filled MOF render it suitable for high energy and/or multiwavelength devices with applications including mid infrared Raman amplification [6], imaging [7] and broadband supercontinuum generation [8]. We anticipate that the efficiency with which these silicon microstructured fibers can be launched into and integrated with existing fiber infrastructures will open up new possibilities for the next generation of silicon photonics devices.

2. Design and fabrication

Pure silica MOFs are fabricated by stacking and fusing arrays of capillaries and rods into preforms a few centimeters in diameter and tens of centimeters in length, which are then drawn at high temperatures to yield structures with hole sizes ranging anywhere from tens of microns down to tens of nanometers, over kilometre lengths [9]. The MOF template used in our investigations was a hollow core silica PBGF where the central core is defined by omitting three of the capillary tubes. This was chosen because of its relatively small core compared to the more typical PBGFs, which have a core formed by either seven or nine omitted cells, and, as a result, this structure has been shown to be single mode over the telecoms band of $1.4-1.7\,\mu$m [10]. A SEM micrograph of the silica template is shown in Fig. 1(a) from which we can measure the core size to be $\sim 9\,\mu$m and the widths of the silica struts as ~ 150 nm.

Infiltration of bulk silicon into the holes of the MOF template is conducted using a high pressure microfluidic chemical deposition technique [4], possible due to the excellent mechanical strength of the MOFs [11]. Using the holes in the MOF as micro reaction chambers, silane is forced to flow through the structure under high pressures and temperatures. The material is deposited in an amorphous state so that it bonds smoothly to the silica walls, minimizing the roughness at the silicon-silica interfaces [12]. Crystallization to polysilicon is conducted after the deposition process by annealing at temperatures up to $\sim 1300\,^{\circ}$C. Fig. 1(b) shows an SEM micrograph of the silicon microstructured fiber cross-section, prepared via hand cleaving, from which we see that despite the difference in the core and cladding hole sizes the silica template has been completely filled. From this image it is also apparent that standard fiber cleaving techniques do not result in a clean fracture across the end face of this composite structure. Thus, to obtain efficient coupling into and out of the silicon microstructured fibers it is necessary to polish the end faces by mounting them inside thicker silica capillary tubes, then using a standard polishing technique. Fig. 1(c) shows an example of a polished fiber imaged using an optical microscope. The distortions seen in the silica webbing are an artifact of the high temperature

#114924 - $15.00 USD Received 28 Jul 2009; revised 28 Aug 2009; accepted 15 Sep 2009; published 23 Sep 2009

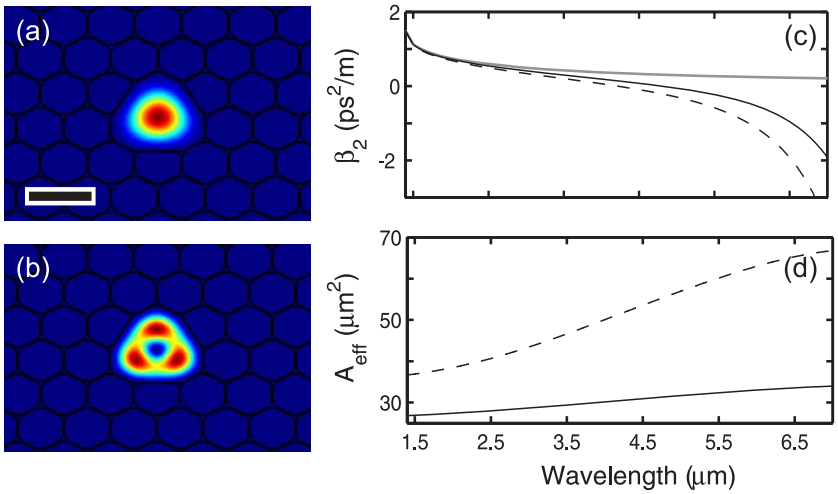

Fig. 2. (a) Fundamental (scale bar $10\,\mu$m) and (b) second order guided modes calculated at $1.55\,\mu$m. (c) Group velocity dispersion of the fundamental (black solid) and second order modes (black dashed) together with the dispersion of bulk silicon (grey solid). (d) Corresponding effective mode area of the fundamental and second order modes as functions of wavelength.

anneal, during which we expect the structures to be subject to mechanical stresses owing to the different thermal properties of the materials.

To investigate the guiding properties of these silicon microstructured fibers we have conducted modal simulations of the structure shown in Figs. 1(b-c), using a full vector finite element method (FEM), where we assume that the grain sizes of the polysilicon sample are sufficiently large that we can approximate the refractive index with that of single crystal silicon. Interestingly, we have found that this structure behaves in a similar manner to a LMA endlessly single mode MOF where the wavelength dependent cladding index changes so to always cut off the second order mode, though in this case the silicon fiber supports two guided modes over the entire low loss wavelength transmission range of silicon $1.2-7\,\mu$m. By defining the effective cladding index to be that of the fundamental space-filling mode [13], we have confirmed that at the shorter (near infrared) wavelengths this index is indeed very close to that of the bulk silicon core index, but decreases for increasing wavelength. The cladding index can then be used to estimate the numerical aperture which is found to be in the range $0.2-0.3$ over the extended telecoms band of $1.3-1.7\,\mu$m, slowly increasing up to ~ 1 at $7\,\mu$m. Fig. 2 shows the fundamental (a) and second order (b) mode profiles together with their calculated group velocity dispersion (GVD) (c) and effective mode areas (d) as functions of wavelength. Due to the large core size, over the near infrared wavelengths the dispersion properties of the fiber are essentially those of the bulk silicon material (solid grey line). However, in the mid infrared waveguide dispersion starts to contribute so that the curves deviate, with the fundamental mode crossing the zero dispersion point at $4.8\,\mu$m. Calculations of the effective mode area reveal that whilst the fundamental mode dimensions only show a weak dependence on the guided wavelength, a characteristic typical of a standard LMA fiber, the second order mode becomes increasingly less confined for the longer wavelengths.

#114924 - $15.00 USD Received 28 Jul 2009; revised 28 Aug 2009; accepted 15 Sep 2009; published 23 Sep 2009

3. Optical characterization

Characterization of the optical transmission properties of a 6 mm length of fiber, annealed up to $\sim 1125\,^{\circ}$C, was conducted using a supercontinuum source over the extended telecoms wavelength range of $1.3-1.7\,\mu$m. The supercontinuum light is filtered using a tunable acousto-optic device to yield an average power of ~ 0.5 mW at each wavelength, and launched into the silicon core via free space coupling using a $25\times$ microscope objective lens. A second $40\times$ objective is used to capture the transmitted light and focus it onto an Electrophysics MicronViewer 7290A infrared camera. Fig. 3 shows the near field mode images for light at (a) $1.3\,\mu$m, (b) $1.55\,\mu$m and (c) $1.7\,\mu$m, where at each wavelength we can clearly distinguish the two allowed modes. Importantly, coupling is preferentially obtained into the fundamental mode, with the second order mode only being isolated when the input beam is launched off-axis to the core. The asymmetries seen in the mode profiles at the shorter wavelengths are most likely due to mixing between the allowed modes, though this may also be due in part to the asymmetry in the microstructured template. At $1.7\,\mu$m the second order mode is more difficult to excite resulting in a higher purity fundamental mode. We note that the isolated node on the left hand side in Fig. 3(c - middle) is a silicon cladding rod mode, coupling into which is hard to avoid owing to the off-axis launch. The right hand column plots the normalized cross section of the fundamental modes (dotted

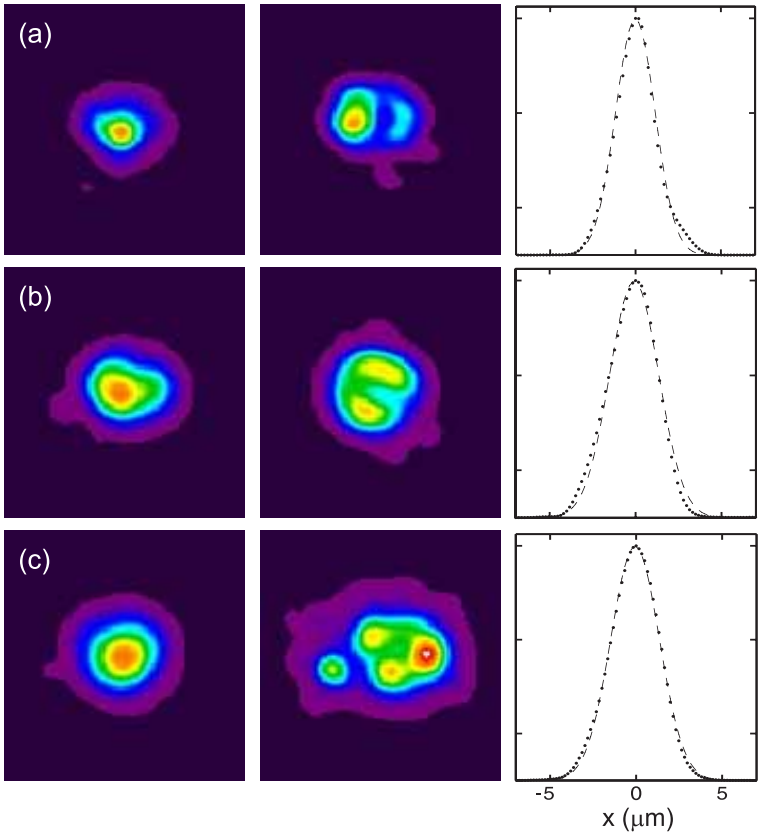

Fig. 3. Intensity profiles of the fundamental (left column) and second order (middle column) modes excited at the input wavelengths: (a) $1.3\,\mu$m, (b) $1.55\,\mu$m and (c) $1.7\,\mu$m. The right column plots the normalized cross sections (dotted lines) together with their Gaussian fits (dashed lines).

#114924 - $15.00 USD Received 28 Jul 2009; revised 28 Aug 2009; accepted 15 Sep 2009; published 23 Sep 2009

curves) showing good agreement with their Gaussian fits (dashed lines). From the full width at half maximum (FWHM) values at the $1/e^2$ power level, we estimate the effective mode areas to be $21\,\mu m^2$, $26\,\mu m^2$ and $26\,\mu m^2$, top to bottom, which match well with the $\sim 27\,\mu m^2$ predicted from the FEM modelling for all the fundamental modes over our wavelength range. This mode area is thus comparable with the effective area of the fundamental mode of a single mode fiber $\sim 70\,\mu m^2$, which is in contrast to those of on-chip devices, typically of nanometer dimensions, that are at least an order of magnitude smaller [3].

Before measuring the transmission losses, micro-Raman measurements were conducted to determine the material quality of the polycrystalline silicon. A 633 nm HeNe laser was focused onto the silicon rods through the side of the transparent silica cladding, with a spot size of $\sim 2\,\mu m$ and ~ 3 mW of power at the outer surface, and the backscattered radiation recorded on a thermoelectrically cooled Horiba Jobin Yvon Synapse CCD detector to yield the spectrum given in the top curve of Fig. 4(a). The spectrum is fitted with a Voigt profile (dashed curve) to account for the $1.7\,cm^{-1}$ Gaussian instrument contribution so that we estimate a Lorentzian FWHM of $3.6\,cm^{-1}$ for the polysilicon wires. Comparing this with the Raman spectrum of a single crystal silicon wafer (Fig. 4(a) - bottom curve) that has a Lorentzian FWHM of $2.7\,cm^{-1}$, the polysilicon peak has a slightly broader linewidth, as expected. This broadening is due to the combined effect of the single crystal grains surrounded by the amorphous silicon filling and can be improved by optimizing the annealing process [14]. From previous depositions with similar linewidths we anticipate the crystal grain sizes to be of the order $0.5-1\,\mu m$ [4, 15]. We note that the slight red shift of the polysilicon peak can be attributed to the tensile stress induced at the silicon-silica boundaries owing to the differences in the thermal expansion of the strongly bonded materials as they cool after annealing [15].

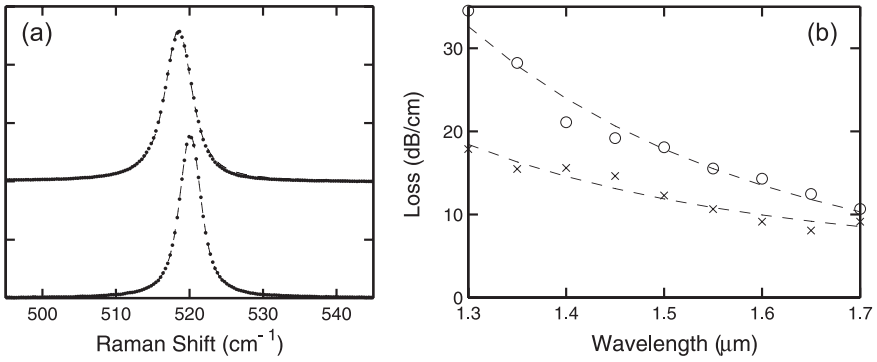

Fig. 4. (a) Micro-Raman spectra of the polysilicon wires in the silica lattice (top) and a single crystal silicon wafer (bottom). Dashed lines are Voigt fits including Gaussian instrument broadening of $1.7\,cm^{-1}$. (b) Transmission losses as a function of wavelength for polysilicon annealed to 1125 °C (○) and 1300 °C (×). Dashed lines are λ^{-4} fits.

Optical transmission losses as a function of the guided wavelength were then determined using a cut-back method, where we polished 1 mm lengths off the sample between each measurement. The supercontinuum source was launched into the fundamental mode as described above, but with the output focused onto a Newport 2832C power meter, and the results are plotted as open circles in Fig. 4(b). From the fitted curve (dashed line) it is clear that this data exhibits a λ^{-4} dependence, in accordance with previous measurements which have indicated that the losses in polysilicon materials are predominantly governed by Rayleigh scattering off the grain boundaries [12, 14]. As this implies that the transmission losses depend largely on the size and quality of the crystal grains, we have measured a second fiber that was annealed up to 1300 °C

#114924 - $15.00 USD Received 28 Jul 2009; revised 28 Aug 2009; accepted 15 Sep 2009; published 23 Sep 2009

to further reduce the local polycrystalline defects. The results, plotted as the crosses in Fig. 4(b), show a significant reduction of the losses, primarily at the shorter wavelengths. Nevertheless, by using the higher temperature anneal we have reduced the losses at 1550 nm by 5 dB/cm to 10 dB/cm, which is in reasonable agreement with the lowest losses measured in a polysilicon core fiber [4]. Further measurements conducted on amorphous silicon microstructured fibers, taken before the high temperature anneal, have confirmed that the losses of these fibers can be primarily attributed to the material quality. Thus by optimizing the time and temperature of the annealing procedure together with the deposition process to improve the polycrystalline quality, or alternatively by modifying the deposition process to obtain high quality low loss hydrogenated amorphous silicon [16], we anticipate that the losses of these silicon microstructured fibers will approach those of the lowest recorded values of around a few dB/cm.

4. Conclusion

We have designed and fabricated a large core, dual mode silicon microstructured fiber using a pure silica photonic bandgap guiding fiber as a 3D template. Using this technique, by modifying the template structure and the silicon filling fraction it should be possible to fabricate LMA silicon fibers for single mode operation. Investigations have shown that these silicon microstructured fibers exhibit similar propagation characteristics to the more traditional index guiding air-silica structures but with the potential to exploit the semiconductor functionality of the silicon core. The large fundamental mode area combined with the low optical losses measured in these fibers facilitates coupling to existing fiber infrastructures, opening up new possibilities for the next generation of silicon photonics devices. Owing to the versatility of the deposition technique, with careful design of the MOF template these novel silicon microstructured fibers can be developed for a wide range of applications encompassing areas such as telecoms, medicine and spectroscopy.

Acknowledgments

The authors acknowledge EPSRC (EP/G028273/1) and NSF (DMR-0806860) for financial support and thank F. Poletti for assistance with the modal simulations. A. C. Peacock is a holder of a Royal Society of Engineering fellowship.

#114924 - $15.00 USD Received 28 Jul 2009; revised 28 Aug 2009; accepted 15 Sep 2009; published 23 Sep 2009